

A Population of Teraelectronvolt Pulsar Wind Nebulae in the H.E.S.S. Galactic Plane Survey

S. KLEPSE¹, S. CARRIGAN², E. DE OÑA WILHELMI^{2,5}, C. DEIL², A. FÖRSTER², V. MARANDON², M. MAYER^{1,3}, K. STYCZ¹, AND K. VALERIUS⁴ FOR THE H.E.S.S. COLLABORATION.

¹ DESY, Platanenallee 6, D-15738 Zeuthen, Germany

² Max-Planck-Institut für Kernphysik, P.O. Box 103980, D-69029 Heidelberg, Germany

³ Institut für Physik und Astronomie, Universität Potsdam, Karl-Liebknecht-Str. 24/25, D-14476 Potsdam-Golm, Germany

⁴ Erlangen Centre for Astroparticle Physics (ECAP), Universität Erlangen-Nürnberg, Erwin-Rommel-Str. 1, D-91058 Erlangen, Germany

⁵ now at: Institut de Ciències de l'Espai (IEEC-CSIC), 08193 Bellaterra, Spain

stefan.klepser@desy.de

Abstract: The most numerous source class that emerged from the H.E.S.S. Galactic Plane Survey are Pulsar Wind Nebulae (PWNe). The 2013 reanalysis of this survey, undertaken after almost 10 years of observations, provides us with the most sensitive and most complete census of gamma-ray PWNe to date. In addition to a uniform analysis of spectral and morphological parameters, for the first time also flux upper limits for energetic young pulsars were extracted from the data. We present a discussion of the correlation between energetic pulsars and TeV objects, and their respective properties. We will put the results in context with the current theoretical understanding of PWNe and evaluate the plausibility of previously non-established PWN candidates.

Keywords: PWN, pulsar wind nebula, population, H.E.S.S.

1 Introduction

The H.E.S.S. Galactic Plane Survey (HGPS) is the first survey of TeV sources in the inner part of the Milky Way. After ten years of data taking and an extensive reanalysis of all data, a full release of a source catalog and skymaps is in preparation [1]. This allows us to make a census of the most frequent source class in this catalog, Pulsar Wind Nebulae (PWNe).

When massive stars explode in a core-collapse supernova, a neutron star can remain as a leftover which is often detected as a pulsar through its pulsations emitted in radio or other wavelengths. This pulsar has an outflow of relativistic electrons and positrons which runs into a termination shock and forms a magnetised plasma around the pulsar. This plasma bubble, which is the PWN, grows and shines for many thousands of years and can reach sizes of tens of parsecs across. The mechanisms by which it emits non-thermal radiation are synchrotron (radio to sub-GeV gamma rays) and inverse Compton radiation (GeV to TeV gamma rays).

The interesting questions that are addressed in the efforts to measure and understand the nature of PWNe are how they evolve spatially and spectrally with time, and how the injection of particles from the pulsar works and evolves. The evolution of a particular PWN strongly depends on the surrounding supernova remnant (SNR), and both the SNR and PWN evolution depend on the surrounding medium and other factors. In this study, where we compare all PWNe detected in the HGPS, we can see the large scatter of PWN properties caused by these different local conditions, while at the same time we investigate common trends in evolution that can be established nevertheless.

2 Correlation of TeV Sources and Young Pulsars

From the many firmly associated PWNe in the online catalog TeVCat¹, and also from previous works on the whole PWN population [2, 3, 4], it can be considered an established fact that young energetic pulsars tend to have a TeV PWN detectable with current instruments, while old, less energetic ones do not. This is also what can be expected from the theoretical viewpoint because old pulsars inject less and less particles and at some point are not able to compensate diffusion and radiative losses anymore. These PWNe are still there, but too faint and/or too extended to be detected with present instruments.

Using the new HGPS reanalysis, we update the study pursued in [2]. Figure 1 shows the fraction of pulsars with a TeV PWN detection as a function of the spin-down power \dot{E} of the pulsar. The TeV detection is evaluated on the H.E.S.S. survey skymap, and the pulsar sample used is that of the Parkes Multibeam Pulsar Survey (PMPS) [6]. To estimate the fraction expected from chance coincidences, the PMPS sample is randomised many times in galactic longitude and latitude independently and for each bin and \dot{E} . The expectation of chance coincidences is displayed as a black line in Fig. 1. The error bars on the data points are calculated with binomial statistics, as described in [5]. As in [2], we also find in this work that pulsars with high \dot{E} are detected more often than can be expected by chance, confirming the previous claims that these pulsars are more likely to have a TeV PWN counterpart than the less energetic ones.

In a similar fashion, this correlation can be demonstrated in a spatial correlation plot (Fig. 2), which shows the distribution of angular distances θ between all PMPS pulsars and all TeV catalog source positions. To evaluate

1. <http://tevcat.uchicago.edu/>

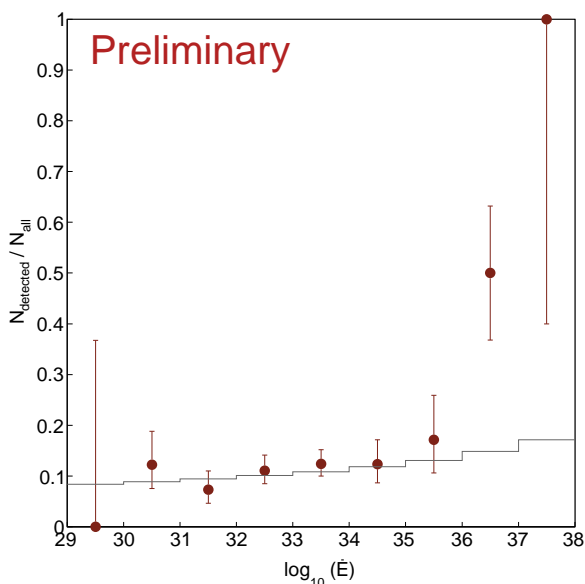


Figure 1: Detection fraction of PMPS pulsars evaluated in bins of \dot{E} . The black histogram at the bottom is the expectation from randomised pulsar populations, see text. The error bar of the highest- \dot{E} bin is large because it is based on only two pulsars.

the expected rate of chance coincidences, the same distribution is again calculated with randomised pulsar populations, shown as a band. At correlation angles of less than about 0.5° , a strong peak is found.

2.1 Candidate Preselection

In the study of the PWN population, which will also evaluate the various unconfirmed PWNe, a two-step candidate selection procedure is applied. First, a very rough *preselection* is made, using rather loose criteria in order not to miss a potential association. TeV sources that are clearly identified as not being a PWN are excluded from this preselection. Secondly, these preselected candidates are discussed in the context of the confirmed PWNe and model predictions. They will be shown in a distinct color in the physics correlation plots in Sec. 3.

Figure 3 shows a preliminary plot of the spin-down powers and characteristic ages of the PWNe and candidates that fulfill the preselection criteria in \dot{E} and angular separation θ . As can be expected, the confirmed PWNe are associated to young and energetic pulsars, whereas the candidates are older and less energetic, making an identification with a TeV source harder to argue.

3 Conclusions on PWN Evolution

PWN evolution is mostly described to happen in three distinct stages: An initial phase of free expansion within the ejecta of the supernova remnant (SNR) shell, a phase of interaction and reverberations of PWN and SNR reverse shock, and finally a relic phase, where pulsar, PWN and SNR might be disconnected from each other and a secondary PWN bubble can form. Most of the known TeV PWNe are in either of the first two phases.

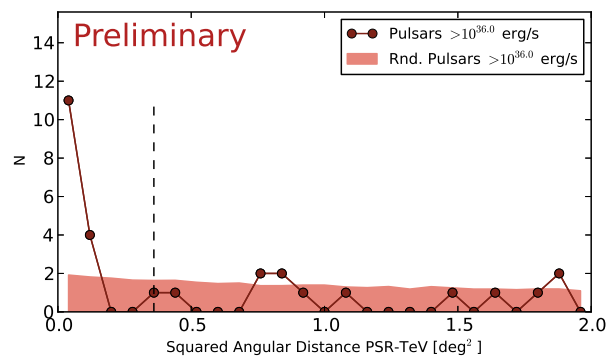


Figure 2: Spatial correlation of high- \dot{E} PMPS pulsars and eligible HGPS source candidates. A clear correlation is seen as a peak at small angular distances, where very few chance coincidences are expected. The dashed line indicates the preliminary criterion to look for preselection candidates, see text.

3.1 General Trends in PWN Modeling

While the free expansion phase was often explored in theory and is comparably well-understood, also thanks to the prominent Crab Nebula, the second phase, where the PWN enters a complex interaction with the SNR reverse shock is still relatively difficult to describe in a quantitatively realistic way. Most of the works either strongly simplify the geometry of the system and/or are done in numerical fashion, making them a case study rather than providing general formulae. We therefore do not attempt to model a full synthetic population of PWNe in the galaxy, but compare the phenomenological trends in the data we have with the common wisdom that can be taken from present theory.

To understand the TeV spectral luminosity of a PWN it is essential to model the electron population in bins of time [9, 10]. Where required, we therefore use a simple, but time-dependent model similar to that outlined in [10] and the formulae therein. To roughly characterise the expected evolution of an average PWN, we assume an initial magnetic field of $50 \mu\text{G}$, and two combinations of initial spin-down time scale τ_0 , initial \dot{E} and braking index n , namely $\tau_0 = 0.5 \text{ kyr}; 5 \times 10^{39} \text{ erg s}^{-1}; n = 3$ (Model 1), and $\tau_0 = 5 \text{ kyr}; 1 \times 10^{39} \text{ erg s}^{-1}; n = 2$ (Model 2). These modelings were chosen to represent two pulsar scenarios with different decay characteristics, and τ_0 and \dot{E}_0 were adjusted for each given n such that the expected evolution curve in characteristic age appears correctly scaled on Fig. 3. In addition to what is described in [10], the model now contains a free expansion phase in its radius evolution, which increases the adiabatic losses in the early evolution. To compensate the efficiency loss implied by that, we increased the lepton conversion efficiency from 0.3 to 1.

3.2 Extension Evolution

The extension of a PWN is theoretically expected to develop as $R_{\text{PWN}} \sim t^{1.2 \dots 0.3}$, with an index depending on the evolutionary state [7, 8]. This radius R_{PWN} refers to a sphere which the PWN bubble is usually assumed to fill isotropically with electron/positron plasma. The absolute scale of the radius evolution depends on the surrounding medium and the SNR evolution and can therefore vary considerably.

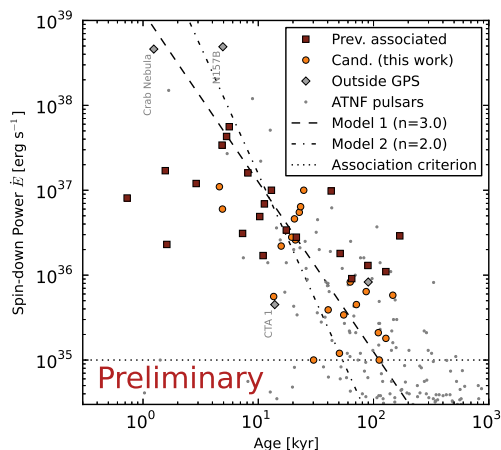


Figure 3: Spin-down power \dot{E} plotted against characteristic age of previously identified PWNe (dark red squares) and preliminary preselection candidates in this work (yellow circles). The grey diamonds are additional PWNe that are not in the HGPS, and the grey dots are other ATNF pulsars for which no TeV counterpart has been detected.

The measurements available are radii defined as the width σ of a two-dimensional Gaussian function instead of a sphere radius. This σ can only be measured if the PWN is bigger than the minimum resolvable extension, which depends on the exposure time and may generally be less than the gamma-ray point spread function. Also, the source has to be sufficiently smaller than the radius of the field of view, such that a background subtraction remains possible. For H.E.S.S., this limits the range of detectable extensions to about 0.03° to 0.6° .

Despite this observational bias and theoretical uncertainty, a rough trend can be observed in Fig. 4. The evolution of radii roughly matches the expected $R_{\text{PWN}} \sim t^{0.3}$ for evolved PWNe that are in interaction with the SNR reverse shock. The model curves in our figures take into account the conversion between true and characteristic age, see [7, 8].

3.3 Efficiency Evolution

The TeV efficiency, defined as the ratio of TeV luminosity and pulsar spin-down power, is often used to argue the plausibility of a PWN association. It is, however, a difficult matter, because the TeV emission is produced by a population of electrons that is summed up over the whole evolution of a PWN, while the spin-down power is a momentary property of a pulsar. It is therefore expected that this apparent efficiency of a PWN can increase with time or even exceed unity.

Figure Fig. 5 shows the evolution of efficiency with characteristic age. Thanks to the many new upper limits we extract from the HGPS skymap, it is clear that while some candidates may exceed an efficiency of 1, most of the PWNe do not reach such a high efficiency. From the modelings we show, one can see that the braking index n , which defines how quickly \dot{E} decreases with time, probably plays an important role in the efficiency evolution. A lower braking index of $n = 2$ leads to less outflow than $n = 3$ and therefore less efficiency. On the other hand, we also find that an even lower n can lead to an artificial boost in efficiency by letting the momentary \dot{E} drop very rapidly

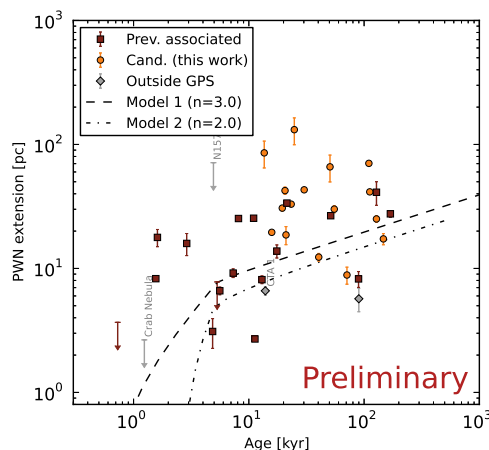


Figure 4: Dependence of measured PWN extensions on characteristic age. The breaks in the models happen at the time when the PWN encounters the SNR reverse shock, which is assumed to happen at 5 kyr (true age, as opposed to characteristic age which is shown in the plot).

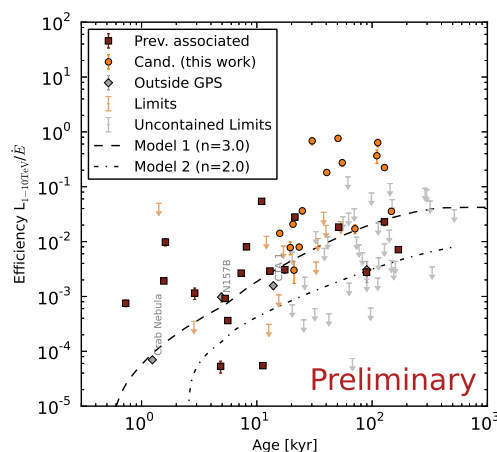


Figure 5: PWN efficiency vs. characteristic age. The yellow limits are likely to enclose the respective PWN, whereas the grey limits are likely to limit only the inner core of it, so the PWN is not fully contained.

(not displayed here). A high efficiency may therefore either indicate a productive particle generation, or just a fast decrease of the pulsar \dot{E} .

4 Summary and Outlook

We presented first excerpts of a study of the TeV PWNe population revealed by the H.E.S.S. Galactic Plane Survey. The study is to be completed using the final catalog, and will contain a discussion of the PWN candidates and more conclusions on the present theoretical understanding of pulsar wind nebulae.

Acknowledgment: The support of the Namibian authorities and of the University of Namibia in facilitating the construction and operation of H.E.S.S. is gratefully acknowledged, as is the support by the German Ministry for Education and Research (BMBF), the Max Planck Society, the German Research Foundation (DFG), the French Ministry for Research, the CNRS-IN2P3

and the Astroparticle Interdisciplinary Programme of the CNRS, the U.K. Science and Technology Facilities Council (STFC), the IPNP of the Charles University, the Czech Science Foundation, the Polish Ministry of Science and Higher Education, the South African Department of Science and Technology and National Research Foundation, and by the University of Namibia. We appreciate the excellent work of the technical support staff in Berlin, Durham, Hamburg, Heidelberg, Palaiseau, Paris, Saclay, and in Namibia in the construction and operation of the equipment.

References

- [1] S. Carrigan et al., this conference, ID XXX
- [2] S. Carrigan, J. A. Hinton, W. Hofmann et al., Proc. ICRC Mérida 2 (2007) 659, arXiv:0709.4094.
- [3] V. Marandon, PhD thesis, Observatoire de Paris, Université Paris 7, 2010
- [4] M. Mayer, Dipl. thesis, Universität Erlangen-Nürnberg, 2010
- [5] S. Carrigan, PhD thesis, Ruperto-Carola University of Heidelberg, 2007
- [6] R. N. Manchester et al., MNRAS 328 (2001) 17
- [7] B. M. Gaensler, P. O. Slane, ARA&A 44 (2006) 17
- [8] S.P. Reynolds, R.A. Chevalier, ApJ 278 (1984) 638
- [9] J. Martín, D. F. Torres, N. Rea, MNRAS 427 (2012) 415
- [10] M. Mayer et al., ArXiv e-prints (2012) 1202.1455